haematologica
Journal of the Ferrata Storti Foundation

IDH1-mutated B-cell acute lymphoblastic leukemia characterized by oncogenic reprogramming of lipid metabolism

by Yu Qian, Dan Shen, Qing Ling, Shuqi Zhao, Yutong Zhou, Yanchun Zhao, Xia Li, Yungui Wang, Jiansong Huang, Jinghan Wang, Wenjuan Yu, Hongyan Tong, Jie Sun, Xiang Zhang and Jie Jin

Received: June 17, 2025.
Accepted: December 22, 2025.

Citation: Yu Qian, Dan Shen, Qing Ling, Shuqi Zhao, Yutong Zhou, Yanchun Zhao, Xia Li, Yungui Wang, Jiansong Huang, Jinghan Wang, Wenjuan Yu, Hongyan Tong, Jie Sun, Xiang Zhang and Jie Jin. IDH1-mutated B-cell acute lymphoblastic leukemia characterized by oncogenic reprogramming of lipid metabolism.
Haematologica. 2026 Jan 8. doi: 10.3324/haematol.2025.288472 [Epub ahead of print]

Title

IDH1-mutated B-cell acute lymphoblastic leukemia characterized by oncogenic reprogramming of lipid metabolism

Running title

*IDH1*mut B-ALL

Authors

Yu Qian[1,2,3,4,*], Dan Shen[1,2,3,4,*], Qing Ling[1,2,3,4,*], Shuqi Zhao[1,2,3,4], Yutong Zhou[1,2,3,4], Yanchun Zhao[1,2,3,4], Xia Li[1,2,3,4], Yungui Wang[1,2,3,4], Jiansong Huang[1,2,3,4], Jinghan Wang[1,2,3,4], Wenjuan Yu[1,2,3,4], Hongyan Tong[1,2,3,4], Jie Sun[1,2,3,4,#], Xiang Zhang[1,2,3,4,#], Jie Jin[1,2,3,4,5,#]

Affiliations

1 Department of Hematology, the First Affiliated Hospital, Zhejiang University School of Medicine, Hangzhou, Zhejiang, PR China

2 Zhejiang Key Laboratory for Precision Diagnosis and Treatment of Hematological Malignancies, Hangzhou, Zhejiang, PR China

3 Zhejiang Provincial Clinical Research Center for Hematological disorders, Hangzhou, Zhejiang, PR China

4 Zhejiang University Cancer Center, Hangzhou, Zhejiang, PR China

5 Jinan Microecological Biomedicine Shandong Laboratory, Jinan, People's Republic of China

*: These Authors equally contributed to the work and share first authorship.

#: Corresponding authors

Jie Sun PhD. Address: Department of Hematology, The First Affiliated Hospital, Zhejiang University College of Medicine, #79 Qingchun Rd, Hangzhou, Zhejiang Province, China 310003; E-mail: sunjiehm@zju.edu.cn; Phone: +86-571-87236575;

Xiang Zhang M.D. Address: Department of Hematology, The First Affiliated Hospital, Zhejiang University College of Medicine, #79 Qingchun Rd, Hangzhou, Zhejiang Province, China 310003; E-mail: hillhardaway@zju.edu.cn; Phone: +86-571-87236898; Fax: +86-571-87236702

Jie Jin M.D. Address: Department of Hematology, The First Affiliated Hospital, Zhejiang University College of Medicine, #79 Qingchun Rd, Hangzhou, Zhejiang Province, China 310003; E-mail: jiej0503@zju.edu.cn; Phone: +86-571-87236702; Fax: +86-571-87236702

Authorship Contributions

J. Jin, X. Zhang and J. Sun designed the research study and supervised the experiments. Y. Qian, D. Shen and Q. Ling performed the research. Y. Wang and J. Huang contributed essential reagents and tools. S. Zhao, Y. Zhou, Y. Zhao and X. Li collected clinical samples and analyzed the data. H. Tong and W. Yu provided advices for this study. Y. Qian and X. Zhang wrote the paper. J. Jin reviewed the paper. All authors read and approved the final manuscript.

Disclosure of Conflicts of Interest

The authors declare that they have no conflict of interest.

Acknowledgements

We would like to thank all members of Department of Hematology, The First Affiliated Hospital to Zhejiang University College of Medicine for their supports. RNA-Sequencing was supported by Oebiotech Company (Shanghai, China) and Acornmed Company (Beijing, China). LC-MS/MS and GC-MS/MS were provided by Shanghai Luming biological technology co., LTD (Shanghai, China).

Funding

This work is supported by Key international cooperation projects of National Natural Science Foundation of China (81820108004, 82200161), National Key Research and Development Program of China (2022YFC2502700, 2022YFC2502701), Research Project of Jinan Microecological Biomedicine Shandong Laboratory (JNL-2022034C), and Natural Science Foundation of Zhejiang Province (MS25H080017).

Data Sharing Statement

The datasets used and/or analyzed during the current study are available from the corresponding author on reasonable request.

B-cell acute lymphoblastic leukemia (B-ALL) is a highly aggressive hematological malignancy with marked genetic heterogeneity, accounting for approximately 75% of adult ALL cases.[1] The ubiquitous application of high-throughput technologies has facilitated the discovery of novel B-ALL molecular subtypes, including *DUX4* and *MEF2D* rearrangements, which have refined risk stratification for affected individuals.[2,3] *Isocitrate dehydrogenase 1* (*IDH1*) mutations, which occur in approximately 8% of acute myeloid leukemia (AML) patients, are comparatively infrequent in B-ALL.[4] *IDH1* mutations have been well-established as key drivers of leukemogenesis through the production of the oncometabolite (R)-2-hydroxyglutarate (R-2HG).[4,5] Although *IDH1*-mutated B-ALL had been documented to display distinct transcriptional signatures and prognostic features, this molecular subtype remains understudied due to its rarity.[6] Previously, we reported a case of *IDH1*-mutated B-ALL characterized by prominent cytoplasmic lipid droplets (LDs) accumulation in leukemic blasts, a morphological phenotype typically associated with ALL-L3 in French-American-British (FAB) classification.[7] Inspired by this observation, we conducted a comprehensive analysis to characterize features of *IDH1*-mutated B-ALL in our cohort, which potentially provided novel insights into its biological properties and potential therapies.

In this study, a total of 30 patients with *IDH1*-mutated B-ALL were enrolled, and additional 188 patients with *IDH1*-WT B-ALL were used as controls. All instances with the characteristic immunophenotype of B-ALL, were newly-diagnosed and enrolled at the First Affiliated Hospital to Zhejiang University School of Medicine (IIT20240358B). All procedures in studies involving human participants were performed in accordance with the ethical standards of the institutional research committee and with the 1964 Helsinki Declaration and its later amendments. Written informed consent was obtained from all participants. *IDH1* mutation testing was performed for all patients, using a combination of Next-Generation Sequencing (NGS) and PCR-based methods. Among the *IDH1*-mutated patients, the mutation sites of the *IDH1* gene were heterogeneous. Specifically, 13 patients had the *R132C* mutation, 9 had the *R132S* mutation, 3 had the *R132G* mutation and for 5 patients, the mutation sites were unavailable (Figure 1A). Baseline characteristics analysis demonstrated that *IDH1*-mutated patients exhibited significantly advanced age at diagnosis (56[26-69] vs. 43[14-85] years, P<0.01). Notably, *IDH1*-mutated patients showed significantly lower white blood cell (WBC) counts (2.6[2.1-3.0] vs. 9.4[3.6-33.0] $\times 10^9$/L, P=0.04) and hemoglobin levels (70[57.5-84.5] vs. 89[67.0-114.3] g/L, P<0.01). For genetic alteration, a significantly lower frequency of *BCR::ABL1* fusion (0% vs. 34.6%, P<0.01) and a significantly higher frequency of *BCOR* (13.3% vs. 1.1%, P<0.01) mutation were found in *IDH1*-mutated patients. Regarding therapeutic outcomes, the *IDH1*-mutated group exhibited lower complete remission (CR) rates (82% vs. 93%, P=0.08), higher relapse rates (53% vs. 30%, P=0.07), and higher mortality rates (32% vs. 16%, P=0.09) compared to the *IDH1*-WT group following standard chemotherapy protocols established by Institute of Hematology and Blood Diseases Hospital, Chinese Academy of Medical Sciences and Peking Union Medical College, Tianjin[8] (Table 1). Consistently, *IDH1*-mutated patients had significantly worse event-free survival (EFS) compared to *IDH1*-WT patients (median 332 days vs 446 days, P=0.02). Meanwhile, patients with *IDH1* mutation also tended to have worse overall survival (OS) and relapse-free survival (RFS) (Figure 1B). Through univariable and multivariable analysis, we found that *IDH1* mutation was an independent prognostic factor for poor EFS (Univariable, HR=1.882 [1.118-3.166], p=0.017; Multivariable, HR=2.126 [1.168-3.867], p=0.014) (Table S1). These findings underscored the

association between *IDH1* mutation and an aggressive clinical phenotype in the B-ALL cohort.

Our initially reported case with *IDH1*-mutated B-ALL presented with prominent cytoplasmic LDs within leukemic blasts at diagnosis, that prompted us to conduct a systematic morphological analysis of B-ALL specimens in our centers. As revealed, cytoplasmic LDs were obviously present in *IDH1*-mutated B-ALL blasts, but were absent or minimal (<5%) in *IDH1*-WT cases in our cohort (Figure 1C). LDs are specialized organelles primarily composed of neutral triglyceride (TG) and encased by a phospholipid monolayer[9], and the accumulation of LDs was reported to be caused by aberrant lipid metabolism, which promoted disease progression and predicted poor outcomes in a variety of cancers[10]. To explore the influence of *IDH1* mutation on lipid metabolism in B-ALL, RNA-seq was conducted to compare the transcriptomic profiles of *IDH1*-mutated (N=7) with *IDH1*-WT bone marrow blasts (N=31). The expression levels of mRNA in sequence data were calculated as RPKM (Reads Per Kilo-base per Million reads). The criteria of differential gene selection were $P<0.05$ and $|\log_2(\text{fold change})|>2$. Gene Set Enrichment Analysis (GSEA) demonstrated significant enrichment of genes related to oxidative phosphorylation, fatty acid metabolism and adipogenesis in *IDH1*-mutated cells, indicating a transcriptional reprogramming toward lipid metabolic activation (Figure 1D). Moreover, serum TG and high-density lipoprotein-cholesterol (HDL-C) levels were significantly elevated in *IDH1*-mutated patients (N=17) compared to *IDH1*-WT patients (N=177) at diagnosis (Figure 1E). These results indicated an aberrant lipid metabolism in *IDH1*-mutated B-ALL cells.

To further explore the correlation between *IDH1* mutation and LDs as well as TG accumulation, we utilized the LDs Assay Kit-Blue from Dojindo Molecular Technologies (Kumamoto, Japan) and the enzymatic TG measurement assay from Applygen Technologies (Beijing, China). Following 24-hour oleic acid (OA, 100μM) treatment[11], as a positive control, both BALL-1 and RS4-11 cell lines displayed significant increases in LD numbers and TG content (Figure S1A-C). R-2HG is the well-known oncometabolite produced by IDH1 mutation.[4,5] Strikingly, both R-2HG and $IDH1^{R132S}$ mutation could significantly augment LD formation and TG biosynthesis (Figure 2A-B, Figure S1D-G). Moreover, AG120 (Ivosidenib, a mutant IDH1 protein inhibitor) treatment significantly reversed the lipid droplet accumulation phenotype (Figure S1H). R-2HG was reported to inhibit growth of IDH wild type AML cells.[12] In contrast to its inhibitory effect in AML cells such as MV4-11, our results demonstrated that R-2HG treatment sustained the proliferation of B-ALL cell lines including BALL-1, REH, and RS4-11 (Figure S2A-C). Furthermore, we ectopically expressed the $IDH1^{R132S}$ mutant in B-ALL cells, using pCDH1-MSCV-MCS-EF1-GreenPuro plasmid vector for lentivirus-mediated stable transfection, and found that $IDH1^{R132S}$ overexpression sustained B-ALL cell proliferation and conferred apoptotic resistance under serum-free culture conditions (Figure 2C, Figure S2D-F). Thus, IDH1 mutation and its oncometabolite R-2HG directly contributed to aberrant lipid metabolism and sustained B-ALL cell proliferation.

To characterize global alterations in lipid-related metabolic profiles, we performed untargeted metabolomic profiling via mass spectrometry in $IDH1^{R132S}$-overexpressed and R-2HG-treated RS4-11 cells. Differentially abundant metabolites were identified using a combination of VIP (variable importance in projection) >1 and $P<0.05$ (Figure 2D). 60 upregulated and 29 downregulated metabolites were identified in $IDH1^{R132S}$-overexpressed cells relative to control

cells. 35 upregulated and 108 downregulated metabolites were identified in R-2HG treated cells relative to DMSO-treated ones. KEGG pathway enrichment analysis revealed significant upregulation of glycerophospholipid metabolism in both of *IDH1*^{R132S}-overexpressed and R-2HG-treated RS4-11 cells (Figure 2E). Glycerophospholipids as well as sphingomyelins are the main components of biological membranes, including LDs. As indicated, enhanced glycerophospholipid metabolism was a key metabolic signature of *IDH1*^{R132S}-mutated B-ALL, which potentially promoted LD formation.

Collectively, this study provides evidence that *IDH1* mutation is a prognostic biomarker predicting poor therapeutic response and adverse clinical outcomes in B-ALL, supporting its role in clinical risk stratification. Previous study by Yasuda et al. identified 7 *IDH1/IDH2*-mutated patients[6], but only 4 of them were included in the subsequent survival analysis. As a result, *IDH1/IDH2* mutation as a predictor for poor prognosis was not conclusive enough in their study. By including a larger number of patients, our analysis has provided robust evidence for the role of *IDH1* mutation in B-ALL. Therapeutically, small-molecule inhibitors targeting mutant IDH1 (e.g., ivosidenib) have demonstrated efficacy in newly diagnosed IDH1-mutated AML.[13] In contrast, clinical data on IDH1 inhibitors in B-ALL remain exceedingly scarce. Our findings position IDH1 mutations and their associated lipid metabolic aberrations as potentially tractable therapeutic targets. A critical future direction will be to evaluate whether integrating IDH1-directed therapy with conventional chemotherapy can improve treatment responses and long-term survival in this patient subset.

A cornerstone of our work is the discovery of pervasive cytoplasmic lipid droplet (LD) accumulation in IDH1-mutated B-ALL blasts—a previously unrecognized morphological hallmark. We propose a lineage-specific model wherein the oncometabolite R-2HG promotes a net gain in lipid storage by driving lipogenesis that surpasses oxidative consumption. This metabolic reprogramming likely stems from the unique B-cell context, where transcription factors such as PAX5 or constitutive kinase signaling may synergistically amplify lipogenic signals.[14] This stands in contrast to IDH1-mutated AML, where R-2HG often cooperates with mutations that favor oxidative metabolism, accounting for the distinct metabolic phenotypes between these malignancies.[15] Notably, IDH1-mutated B-ALL may converge with ALL-L3 through shared MYC activation, providing a parallel route to LD accumulation.[7] Functionally, we posit that these LDs are not passive reservoirs but active organelles integral to leukemic pathobiology. They may serve as a readily available energy source, modulate membrane fluidity and signaling, and critically, buffer against oxidative stress and ferroptosis—a multifaceted role that represents a compelling avenue for future investigation.

While our findings establish a strong association between IDH1 mutation and LD accumulation, they do not elucidate the underlying causal relationship. Therefore, it remains to be determined whether the aberrant lipid metabolism actively drives LD biogenesis or merely occurs in parallel. Directly testing these competing hypotheses through isotopic tracing and genetic rescue experiments will be an important objective for future work.

References

1. Huguet F, Chevret S, Leguay T, et al. Intensified Therapy of Acute Lymphoblastic Leukemia in Adults: Report of the Randomized GRAALL-2005 Clinical Trial. J Clin Oncol. 2018;36(24):2514-2523.
2. Gu Z, Churchman M, Roberts K, et al. Genomic analyses identify recurrent MEF2D fusions in acute lymphoblastic leukaemia. Nat Commun. 2016;7:13331.
3. Zhang J, McCastlain K, Yoshihara H, et al. Deregulation of DUX4 and ERG in acute lymphoblastic leukemia. Nat Genet. 2016;48(12):1481-1489.
4. Issa GC, DiNardo CD. Acute myeloid leukemia with IDH1 and IDH2 mutations: 2021 treatment algorithm. Blood Cancer J. 2021;11(6):107.
5. Dang L, Yen K, Attar EC. IDH mutations in cancer and progress toward development of targeted therapeutics. Ann Oncol. 2016;27(4):599-608.
6. Yasuda T, Sanada M, Kawazu M, et al. Two novel high-risk adult B-cell acute lymphoblastic leukemia subtypes with high expression of CDX2 and IDH1/2 mutations. Blood. 2022;139(12):1850-1862.
7. Zhang X, Suo S, Wang J, Jin J, Yu W. IDH1R132S -mutated acute lymphoblastic leukaemia resembles Burkitt lymphoma/leukaemia via activating MYC. Br J Haematol. 2021;192(2):e44-e47.
8. Hematology Oncology Committee, Chinese Anti-Cancer Association; Leukemia & Lymphoma Group, Chinese Society of Hematology, Chinese Medical Association. [Chinese guidelines for diagnosis and treatment of adult acute lymphoblastic leukemia (2021)]. Zhonghua xue ye xue za zhi. 2021;42(9):705-716.
9. Goodman JM. The gregarious lipid droplet. J Biol Chem. 2008;283(42):28005-28009.
10. Currie E, Schulze A, Zechner R, Walther TC, Farese RV. Cellular fatty acid metabolism and cancer. Cell Metab. 2013;18(2):153-161.
11. Yang A, Mottillo EP, Mladenovic-Lucas L, Zhou L, Granneman JG. Dynamic interactions of ABHD5 with PNPLA3 regulate triacylglycerol metabolism in brown adipocytes. Nat Metab. 2019;1(5):560-569.
12. Su R, Dong L, Li C, et al. R-2HG Exhibits Anti-tumor Activity by Targeting FTO/m6A/MYC/CEBPA Signaling. Cell. 2018;172(1-2):90-105.e23.
13. Roboz GJ, DiNardo CD, Stein EM, et al. Ivosidenib induces deep durable remissions in patients with newly diagnosed IDH1-mutant acute myeloid leukemia. Blood. 2020;135(7):463-471.
14. Gu Z, Churchman ML, Roberts KG, et al. PAX5-driven subtypes of B-progenitor acute lymphoblastic leukemia. Nat Genet. 2019;51(2):296-307.
15. Thomas D, Wu M, Nakauchi Y, et al. Dysregulated Lipid Synthesis by Oncogenic IDH1 Mutation Is a Targetable Synthetic Lethal Vulnerability. Cancer Discov. 2023;13(2):496-515.

Table 1. Baseline Characteristics of *IDH1*-mutated and WT B-ALL

	B-ALL Categories (N=218)		
	IDH1-mutated	*IDH1*-WT	p-value
N	30	188	
Median age (range), y	56 (26-69)	43 (14-85)	<0.01
<35 y	2 (7%)	80 (43%)	
≥35 y	28 (93%)	108 (57%)	
Gender			0.33
Female	17 (57%)	87 (46%)	
Male	13 (43%)	101 (54%)	
White blood cells count (IQR), $\times 10^9$/L	2.6 (2.1-3.0)	9.4 (3.6-33.0)	0.04
Platelet count (IQR), $\times 10^9$/L	100 (79.5-129.5)	59 (30.5-131.0)	0.75
Hemoglobin (IQR), g/L	70 (57.5-84.5)	89 (67.0-114.3)	<0.01
Bone marrow blast (IQR), %	74 (61.0-88.8)	82 (66.0-90.0)	0.42
Cytogenetic features			0.31
Diploid	20 (91%)	126 (78%)	
Hyperdiploid	2 (9%)	24 (15%)	
Hypodiploid	0	11 (7%)	
Molecular features			
BCR::ABL1	0	65 (34.6%)	<0.01
KMT2A::AFF1	0	4 (2.1%)	>0.99
TCF3::PBX1	0	7 (3.7%)	0.60
TP53 mutation	3 (10%)	16 (8.5%)	0.73
BCOR mutation	4 (13.3%)	2 (1.1%)	<0.01
KMT2A mutation	2 (6.7%)	2 (1.1%)	0.09
DNMT3A mutation	2 (6.7%)	3 (1.6%)	0.14
NRAS mutation	0	21 (11.2%)	0.09
KRAS mutation	0	16 (8.5%)	0.14
Therapeutic outcomes			
Complete remission rate, n (%)	18 (82%)	169 (93%)	0.08
Minimal residual disease negative rate, n (%)	15 (79%)	141 (81%)	0.76
Relapse rate, n (%)	10 (53%)	54 (30%)	0.07
Mortality rate, n (%)	8 (32%)	31 (16%)	0.09
Bone marrow transplantation, n (%)	7 (23%)	79 (42%)	0.07

Figure legend

Figure 1. Characteristics of *IDH1*-mutated B-ALL patients. A. Mutation types of *IDH1* gene in our B-ALL patients. B. Kaplan-Meier analysis of EFS, RFS and OS for *IDH1*-mutated B-ALL patients. C. Representative bone marrow morphology of *IDH1*-mutated (P1-P3) and *IDH1*-WT (C1-C3) B-ALL patients. Red arrows indicate the locations of prominent lipid droplets. D. GSEA for the oxidative phosphorylation, fatty acid metabolism and adipogenesis pathways in *IDH1*-mutated vs. *IDH1*-WT B-ALL samples. E. The serum TG and HDL-C levels of *IDH1*-mutated vs. *IDH1*-WT B-ALL patients at diagnosis. *, $p < 0.05$, **, $p < 0.01$, ***, $p < 0.001$.

Figure 2. *IDH1*^{R132S} conferred an oncogenic reprogramming of lipid metabolism in B-ALL cell lines. A. LDs were stained with Lipi-Blue dye and measured by FCM. The bar graph represented the mean fluorescence intensity of cells stained with Lipi-Blue dye. B. TG levels were detected in B-ALL cells with *IDH1*^{R132S} mutation. C. Starvation (remove FBS for 72h)-induced apoptosis was detected in *IDH1*^{R132S}-overexpressed B-ALL cell lines. The representative FCM analysis of REH cells was shown: gating with the equivalent GFP positivity, cells for the vector control group (n=8000) and IDH1-mutant group (n=5000) were analyzed for apoptosis. D. Dysregulated cell metabolites were analyzed by LC-MS/MS & GC-MS/MS in *IDH1*^{R132S}-mutated vs. vector cells or R-2HG-treated vs. DMSO-treated cells. E. KEGG pathway analysis was conducted for upregulated cell metabolites in *IDH1*^{R132S}-mutated or R-2HG-treated groups were presented. Data are presented as mean ± SEM from three independent experiments (n=3). *, $p < 0.05$, **, $p < 0.01$, ***, $p < 0.001$.

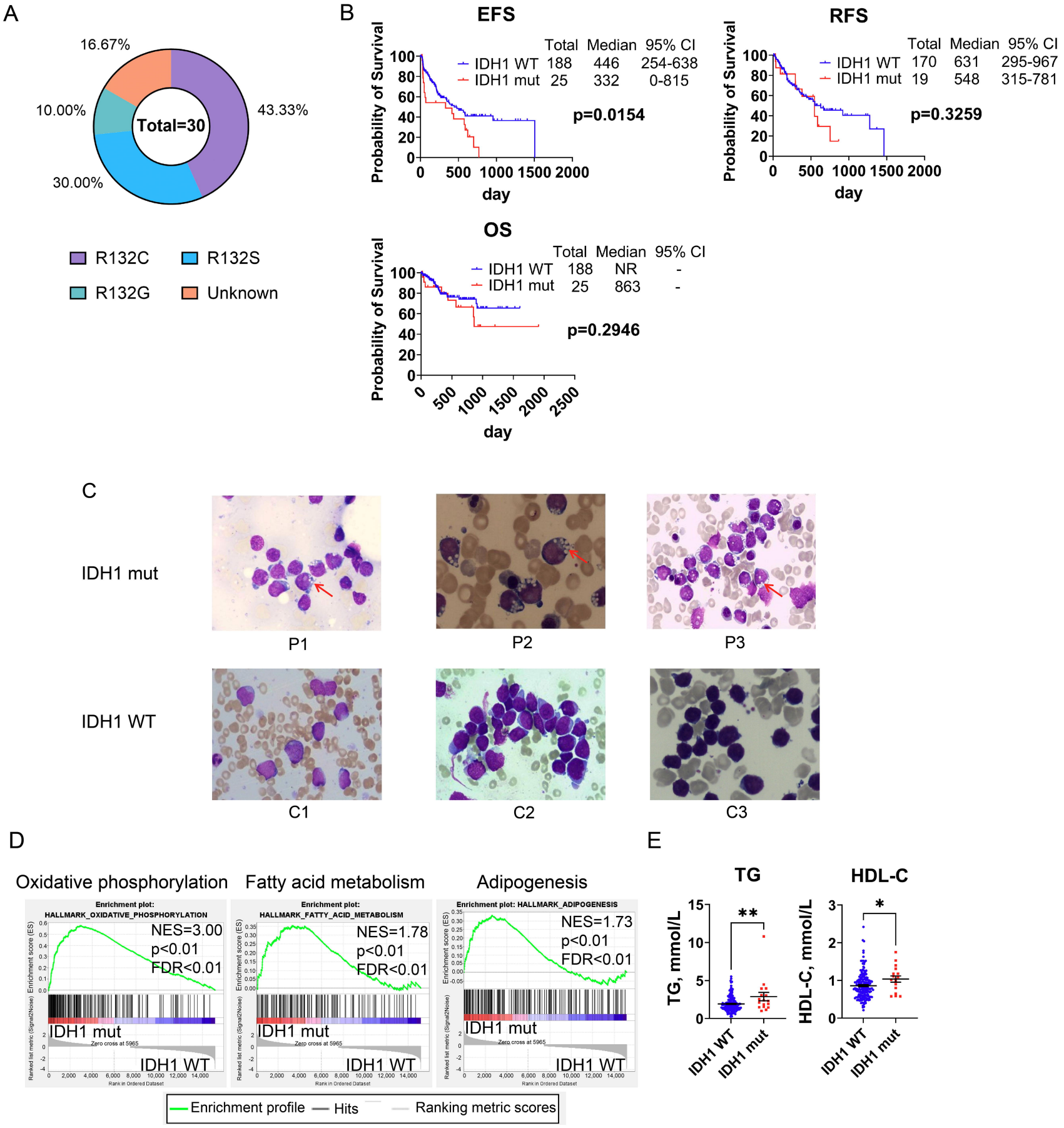
A
16.67%
10.00%
43.33%
30.00%
Total=30
R132C
R132S
R132G
Unknown
B
EFS
Total Median 95% CI
IDH1 WT 188 446 254-638
IDH1 mut 25 332 0-815
p=0.0154
Probability of Survival
day
RFS
Total Median 95% CI
IDH1 WT 170 631 295-967
IDH1 mut 19 548 315-781
p=0.3259
OS
Total Median 95% CI
IDH1 WT 188 NR -
IDH1 mut 25 863 -
p=0.2946
C
IDH1 mut
IDH1 WT
P1
P2
P3
C1
C2
C3
D
Oxidative phosphorylation
Fatty acid metabolism
Adipogenesis
Enrichment plot: HALLMARK_OXIDATIVE_PHOSPHORYLATION
NES=3.00
p<0.01
FDR<0.01
Enrichment plot: HALLMARK_FATTY_ACID_METABOLISM
NES=1.78
p<0.01
FDR<0.01
Enrichment plot: HALLMARK_ADIPOGENESIS
NES=1.73
p<0.01
FDR<0.01
IDH1 mut
Zero cross at 5965
IDH1 WT
Rank in Ordered Dataset
Enrichment profile
Hits
Ranking metric scores
E
TG
HDL-C
TG, mmol/L
HDL-C, mmol/L
**
*
IDH1 WT
IDH1 mut

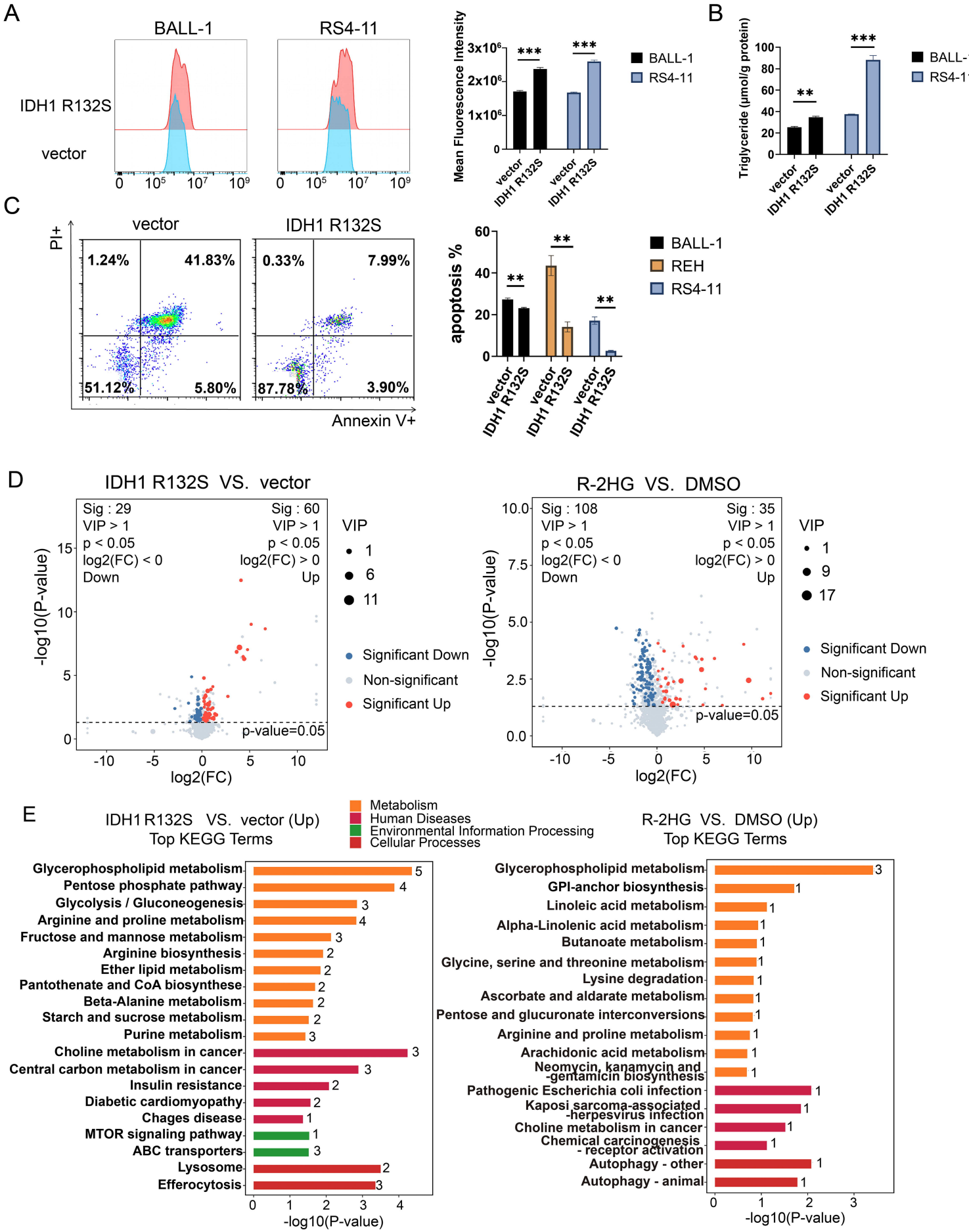
A
BALL-1
RS4-11
IDH1 R132S
vector
Mean Fluorescence Intensity
BALL-1
RS4-11
B
Triglyceride (μmol/g protein)
C
vector
IDH1 R132S
PI+
Annexin V+
1.24%
41.83%
51.12%
5.80%
0.33%
7.99%
87.78%
3.90%
apoptosis %
BALL-1
REH
RS4-11
D
IDH1 R132S VS. vector
Sig : 29
VIP > 1
p < 0.05
log2(FC) < 0
Down
Sig : 60
VIP > 1
p < 0.05
log2(FC) > 0
Up
VIP
Significant Down
Non-significant
Significant Up
p-value=0.05
-log10(P-value)
log2(FC)
R-2HG VS. DMSO
Sig : 108
Sig : 35
E
IDH1 R132S VS. vector (Up)
Top KEGG Terms
Metabolism
Human Diseases
Environmental Information Processing
Cellular Processes
Glycerophospholipid metabolism
Pentose phosphate pathway
Glycolysis / Gluconeogenesis
Arginine and proline metabolism
Fructose and mannose metabolism
Arginine biosynthesis
Ether lipid metabolism
Pantothenate and CoA biosynthese
Beta-Alanine metabolism
Starch and sucrose metabolism
Purine metabolism
Choline metabolism in cancer
Central carbon metabolism in cancer
Insulin resistance
Diabetic cardiomyopathy
Chages disease
MTOR signaling pathway
ABC transporters
Lysosome
Efferocytosis
-log10(P-value)
R-2HG VS. DMSO (Up)
Top KEGG Terms
Glycerophospholipid metabolism
GPI-anchor biosynthesis
Linoleic acid metabolism
Alpha-Linolenic acid metabolism
Butanoate metabolism
Glycine, serine and threonine metabolism
Lysine degradation
Ascorbate and aldarate metabolism
Pentose and glucuronate interconversions
Arginine and proline metabolism
Arachidonic acid metabolism
Neomycin, kanamycin and -gentamicin biosynthesis
Pathogenic Escherichia coli infection
Kaposi sarcoma-associated -herpesvirus infection
Choline metabolism in cancer
Chemical carcinogenesis - receptor activation
Autophagy - other
Autophagy - animal
-log10(P-value)

Supplementary information

Table S1. Univariate and multivariate analysis for EFS in B-ALL.

Parameter	EFS					
	Univariate			Multivariate		
	P	HR	95%CI	P	HR	95%CI
IDH1 (mutated vs. WT)	0.017	1.882	1.118-3.166	0.013	2.199	1.181-4.095
TP53 (mutated vs. WT)	0.127	1.604	0.874-2.942	0.166	1.582	0.827-3.027
NRAS (mutated vs. WT)	0.582	1.194	0.636-2.240	0.387	1.366	0.673-2.773
KRAS (mutated vs. WT)	0.285	1.456	0.732-2.896	0.143	1.781	0.822-3.858
Age (≥35 vs. <35 years)	0.164	1.353	0.884-2.070	0.418	1.220	0.754-1.975
Gender (male vs. female)	0.569	1.125	0.749-1.690	0.953	1.013	0.664-1.546
WBC (≥30 vs. <30 $\times 10^9$/L)	0.050	1.575	1.000-2.479	0.006	2.035	1.231-3.366
HB (≥100 vs. <100 g/L)	0.652	0.908	0.596-1.383	0.978	1.006	0.649-1.560
PLT (100 vs. <100 $\times 10^9$/L)	0.550	0.876	0.569-1.350	0.477	0.853	0.550-1.323

Supplementary Figure legend

Figure S1. LDs was induced by OA and R-2HG in B-ALL cell lines. A. After BALL-1 and RS4-11 were treated with OA (100μM) or DMSO for 24h, LDs were stained with Lipi-Blue dye. The bar graph represented the mean fluorescence intensity of cells stained with Lipi-Blue dye. B. The TG levels were measured in B-ALL cells with 24-hour treatment of OA (100μM) or DMSO. C. Wright-Giemsa staining of BALL-1 and RS4-11 cells treated with OA (100μM) or DMSO for 24h was captured at 400× magnifications. Red arrows indicate the locations of prominent lipid droplets. D. LDs were stained with Lipi-Blue dye in BALL-1 and RS4-11 cells treated with R-2HG (300μM) or DMSO for 24h. The bar graph represented the mean fluorescence intensity of cells stained with Lipi-Blue dye. E. TG measurement in B-ALL cells with 24-hour treatment of R-2HG (300μM) or DMSO. F. Wright-Giemsa staining of BALL-1 and RS4-11 cells treated with R-2HG (300μM) or DMSO for 24h was captured at 400× magnifications. Red arrows indicate the locations of prominent lipid droplets. G. Wright-Giemsa staining of $IDH1^{R132S}$-overexpressed BALL-1 and RS4-11 cells was captured at 400× magnifications. Red arrows indicate the locations of prominent lipid droplets. H. $IDH1^{R132S}$-overexpressed BALL-1 and RS4-11 cells were treated with AG120 (500nM) or DMSO for 24h, LDs were stained with Lipi-Blue dye. The bar graph represented the mean fluorescence intensity of cells stained with Lipi-Blue dye. Data are presented as mean ± SEM from three independent experiments (n=3). *$p < 0.05$, **$p < 0.01$, ***$p < 0.001$.`

Figure S2. Impacts of R-2HG and *IDH1*^{R132S} mutation on the proliferation of B-ALL cell lines. A. B-ALL cell lines (BALL-1, REH and RS4-11) and AML cell line (MV4-11) were treated with different concentrations of R-2HG for 96h and cell viability was analyzed. B. Proliferation curve was draw for B-ALL cell lines and MV4-11 treated with R-2HG (300μM) or DMSO. C. Apoptotic analysis was conducted after B-ALL cell lines were treated with R-2HG (300μM) or DMSO for 96h. D. Western blot detected mutant IDH1 in *IDH1*^{R132S}-overexpressed B-ALL cell lines. E. Proliferation curve was draw for B-ALL cell lines transfected with *IDH1*^{R132S} mutants. F. Apoptosis was detected in *IDH1*^{R132S}-overexpressed B-ALL cell lines supplemented by 10% FBS for 72h. The representative FCM analysis of REH cells was shown. Data are presented as mean ± SEM from three independent experiments (n=3). *$p < 0.05$, **$p < 0.01$, ***$p < 0.001$, ns = no significance.

Figure S1

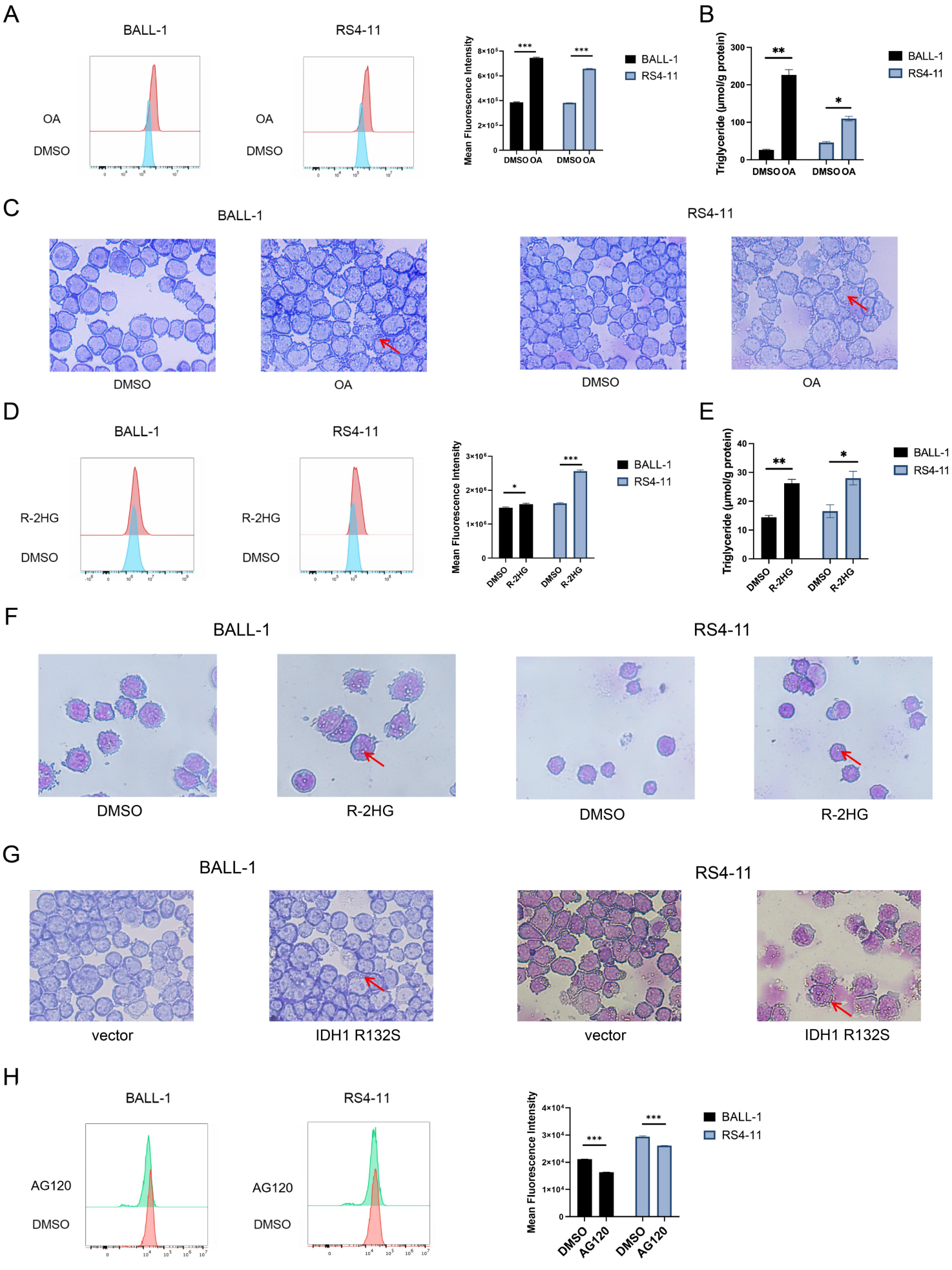
A
BALL-1
RS4-11
OA
DMSO
Mean Fluorescence Intensity
BALL-1
RS4-11
DMSO OA
B
Triglyceride (μmol/g protein)
C
BALL-1
RS4-11
DMSO
OA
D
R-2HG
E
F
G
vector
IDH1 R132S
H
AG120

Figure S2

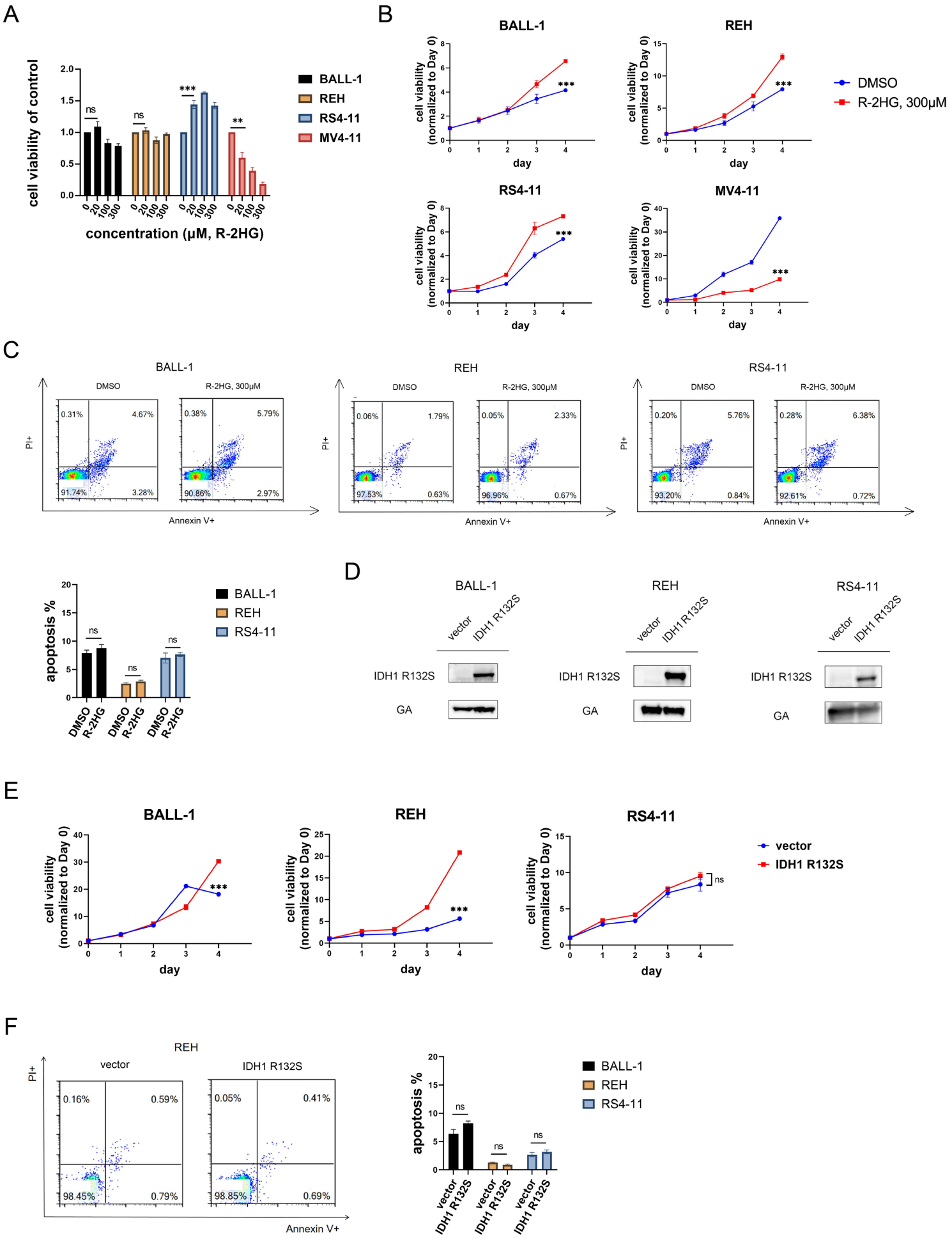
A
cell viability of control
concentration (μM, R-2HG)
BALL-1
REH
RS4-11
MV4-11
B
BALL-1
REH
RS4-11
MV4-11
cell viability (normalized to Day 0)
day
DMSO
R-2HG, 300μM
C
BALL-1
REH
RS4-11
DMSO
R-2HG, 300μM
PI+
Annexin V+
0.31%
4.67%
91.74%
3.28%
0.38%
5.79%
90.86%
2.97%
0.06%
1.79%
97.53%
0.63%
0.05%
2.33%
96.96%
0.67%
0.20%
5.76%
93.20%
0.84%
0.28%
6.38%
92.61%
0.72%
apoptosis %
D
vector
IDH1 R132S
GA
E
F
REH
vector
IDH1 R132S
0.16%
0.59%
98.45%
0.79%
0.05%
0.41%
98.85%
0.69%